Depth Reduction Factor Assessment for Evaluation of Cyclic Stress Ratio Based on Site Response Analysis

Farzad Farrokhzad

Department of Civil Engineering, Babol University of Technology

Abstract

Earthquake properties that affect the liquefaction of a soil are described with one parameter known as the cyclic stress ratio (CSR). The stress reduction coefficient parameter accounts for the flexibility of the soil profile. The previous proposed equations could be used in routine engineering practice so long as the simplified (r_d) was used to assess CSR, but could be unconservative if used in sites with complex soil layers or in design of vital facilities such as dams, hospitals, bridges and . . . .

This research presents the results of studies in Babol city to develop, depth reduction factor (r_d) based on equivalent linear analysis of study area for evaluation of cyclic stress ratio. As a part of microzonation study for the Babol city a total of 35 boreholes have been drilled in 35 km^2 of the research area. The depths of these boreholes ranged about 25 to 35 m. SPT blow counts were taken in each 2 m depth. Many geophysical investigations, generally 35 downhole logging surveys, are carried out in 35 mentioned boreholes for generation and measurement of shear wave velocity. Based on these analyses, the (r_d) diagrams and equations are developed for each mentioned zone.

Keywords Depth reduction Factor (r_d), Liquefaction, Site response analysis, Cyclic shear stress, Earthquake return period, Microzonation

1 Introduction

In geology, a fault is a planar fracture or discontinuity in a volume of rock, across which there has been significant displacement along the fractures as a result of earth movement [1]. An earthquake is caused by a sudden slip on a fault [2]. Stresses in the earth's outer layer push the sides of the fault together [3]. Stress builds up and the rocks slips suddenly, releasing energy in waves that travel through the earth's crust and cause the shaking that we feel during an earthquake [4]. The site safety during earthquakes is related with geotechnical phenomena such as amplification, liquefaction, landsliding and fault movements [5]. Loose sand and silt that is saturated with water can behave like a liquid when shaken by an earthquake [6]. Soil liquefaction describes a phenomenon whereby a saturated or partially saturated soil substantially loses strength and stiffness in response to an applied stress, usually earthquake shaking or other sudden change in stress condition, causing it to behave like a liquid [7]. Evaluation of liquefaction potential requires comparison of the anticipated level of loading imposed on a

soil profile with the inherent resistance of the soil profile to liquefaction [8]. That procedure essentially compares the cyclic resistance ratio (CRR) [the cyclic stress ratio required to induce liquefaction for a cohesionless soil stratum at a given depth] with the earthquake-induced cyclic stress ratio (CSR) at that depth from a specified design earthquake [defined by a peak ground surface acceleration and an associated earthquake moment magnitude] [9]. During an earthquake, the soils will be subject to cyclic shear stresses induced by the ground shaking. The average cyclic stress ratio (CSR) during an earthquake may be estimated by the following Equation 1 [10-14]:

$$CSR = \frac{\tau_{ave}}{\sigma_0'} = 0.65(\frac{a_{max}}{g})(\frac{\sigma_0}{\sigma_0'}).r_d \tag{1}$$

Where a_{max} = maximum acceleration at the ground surface, σ_0 = total overburden pressure at depth under consideration, $\sigma_0{}'$ = effective overburden pressure at depth under consideration and r_d = stress reduction coefficient.

Seed and Idriss considered a soil column as a rigid body [15]. In reality, soil behaves as a deformable body instead of as a rigid body. Hence, the rigid body shear stress should be reduced with a correction factor to give the deformable body shear stress (τ_{max})d [16-18]. This correction factor is called the stress reduction coefficient (r_d) and can be computed as follows:

Values of r_d are commonly estimated from the diagram which is proposed by Seed and Idriss in 1971 (Fig. 1). This chart was determined analytically using a variety of earthquake motions and soil conditions. Average r_d values in the diagram can be estimated using the following functions (Equation 2) [19].

$$\begin{aligned} r_d &= 1 - 0.00765z \quad && For \quad z \leq 9.15(m) \\ r_d &= 1.174 - 0.0267z \quad && For \quad 9.15(m) < z \leq 23(m) \\ r_d &= 0.774 - 0.008z \quad && For \quad 23(m) < z \leq 30(m) \end{aligned} \tag{2}$$

Also, Equation 3 shows the suggestion of Blake [20]

$$r_d = \frac{1 - 0.4113z^{0.5} + 0.04052z + 0.001753z^{1.5}}{1 - 0.4177z^{0.5} + 0.05729z - 0.006205z^{1.5} + 0.00121z^2} \tag{3}$$

Regarding to the research of Golesorkhi , statistically based r_d curves were developed for different earthquake magnitude ranges [21]. The initial study of Golesorkhi has been further extended by Idriss and Golesorkhi.

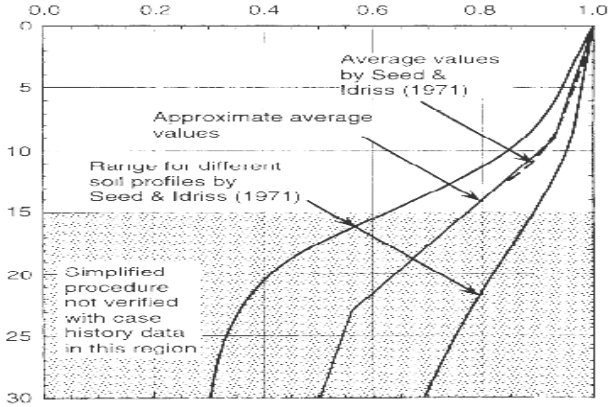

Fig. 1 r_d results from response analyses for 2153 combinations of site conditions and ground motions, superimposed with heavier lines (Seed and Idriss 1971)

The proposed correlation for estimation of r_d as a function of depth, magnitude, intensity of shaking, and site stiffness is presented in Equation 4.

$$\begin{aligned} &In(r_d) = \alpha(z) + \beta(z).M_w \\ &\alpha(z) = -1.012 - 1.126.sin(\frac{z}{38.5} + 5.133) \\ &\beta(z) = 0.106 + 0.118.sin(\frac{z}{37.0} + 5.142) \\ &(z \ = \ depth \ in \ feet) \end{aligned} \tag{4}$$

$$\begin{aligned} &r_d(d, M_W, a_{max}, V^*_{S,12m}) = \qquad For\ d < 65(ft) \\ &\frac{\left[1 + \frac{-23.013 - 2.949a_{max} + 0.999M_W + 0.016V^*_{S,40'}}{16.258 + 0.201e^{0.104(-d + 0.0785V^*_{S,40'} + 24.888)}}\right]}{\left[1 + \frac{-23.013 - 2.949a_{max} + 0.999M_W + 0.016V^*_{S,12m}}{16.258 + 0.201e^{0.104(0.0785V^*_{S,40'} + 24.888)}}\right]} \pm \sigma_{\varepsilon_{rd}} \\ &r_d(d, M_W, a_{max}, V^*_{S,12m}) = \qquad For\ d \geq 65(ft) \\ &\frac{\left[1 + \frac{-23.013 - 2.949a_{max} + 0.999M_W + 0.016V^*_{S,40'}}{16.258 + 0.201e^{0.104(-d + 0.0785V^*_{S,40'} + 24.888)}}\right]}{\left[1 + \frac{-23.013 - 2.949a_{max} + 0.999M_W + 0.016V^*_{S,12m}}{16.258 + 0.201e^{0.104(0.0785V^*_{S,40'} + 24.888)}}\right]} \\ &- 0.0014(d - 65) \pm \sigma_{\varepsilon_{rd}} \end{aligned} \tag{5}$$

$$\sigma_{\varepsilon_{rd}} = \begin{cases} 0.0072d^{0.850} & d < 40ft \\ 0.007240d^{0.850} & d \geq 40ft \end{cases}$$

Cetin et al recognized that r_d is a function of site response, and developed a new correlation for estimation of r_d. The proposed correlation is presented in Equation 5 [22].

Numerous seismic events around study area, such as Manjil-Rudbar earthquake on June 21, 1990, Mazandaran earthquake on May 28, 2004, Tabas earthquake on September 16, 1978 and Bam earthquake on December 26, 2003 have demonstrated the relevance of subsurface soil layers and geotechnical conditions on seismic ground response [23-25]. Equivalent-linear ground response modeling is by far the most commonly utilized procedure in practice [26]. Equivalent-linear soil material modeling is widely used in practice to simulate true nonlinear soil behavior for applications such as ground response analyses [27-28]. The advantages of equivalent-linear modeling include small computational effort and few input parameters. In equivalent linear model, the soil stiffness G is modified in response to computed strains and G and ξ degradation curves. Ground motion is computed for selected G and ξ pair at each layer; in particular, strain histories are calculated; From above effective shear strain γ_{eff} is calculated; From obtained effective shear strain, new pair of G(γ) and $\xi(\gamma)$ are selected using the degradation curves; These steps are repeated until the maximum difference between computed shear modulus and damping ratio values in two successive iterations be less than ~5% [29-31]. In the research of Ishibashi and zhang, equivalent shear moduli and damping ratios for sandy soils were collected and Equation 6 was proposed to best fit data points [32].

$$\begin{aligned}
&\frac{G}{G_{max}} = K(\gamma, I_p)\bar{\sigma}_0^{m(\gamma,I_p)-m_0} \\
&k(\gamma.I_p) = 0.5\left\{1 + tanh\left[ln(\frac{0.000102+n(I_p)}{\gamma})^{0.492}\right]\right\} \\
&m(\gamma, I_p) - m_0 = 0.272\left\{1 - tanh\left[ln(\frac{0.000556}{\gamma})^{0.4}\right]\right\} e^{-0.0145I_p^{13}} \\
&n(I_p) = \begin{cases} 0 & for\ I_p = 0 & Sandy\ soils \\ 3.37\times10^{-6}I_p^{1.404} & for\ 0 < I_p \le 15 & Low\ plastic\ soils \\ 7\times10^{-7}I_p^{1.976} & for\ 15 < I_p \le 70 & Medium\ plastic\ soils \\ 2.7\times10^{-5}I_p^{1.115} & for\ I_p > 70 & High\ plastic\ soils \end{cases}
\end{aligned} \tag{6}$$

2 Study Area

Babol is located in the in the north of Iran, between the northern slopes of the Alborz Mountains and approximately 20 kilometers south of Caspian Sea on the west bank of Babolrud river and receives abundant annual rainfall. Iranian tectonic plate in Middle East affects the seism tectonic condition of Babol (Figure 2) [33-34]. The tectonic environment near Babol city is unusually complicated. Khazar and North Alborz faults are the most significant faults around the study

area (Figure 3). These faults are directed E-NE and W-SW. The Khazar fault is the boundary between the Caspian plain and Alborz Mountain (Figure 4, Figure 5). Table 1 presents a list of active faults affecting the Babol city [35].

Regarding to seismicity of Mazandaran, it can be assumed that for large earthquakes, the faulting process primarily involves repeated breaking of the same fault segment rather than creation of a new fault surface. Table 2 shows recent major earthquakes that are felt in the zone (648584 E, 4049660 N) and (652032 E, 4043901 N). This zone closely bounds Babol city. Also, magnitude distribution of earthquakes in the range of 200 km around the Babol city are presented in Figure 6.

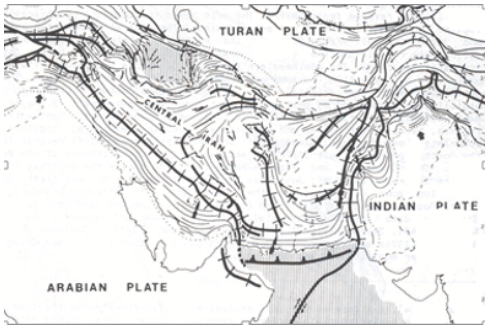

Fig. 2 Tectonic of Study area

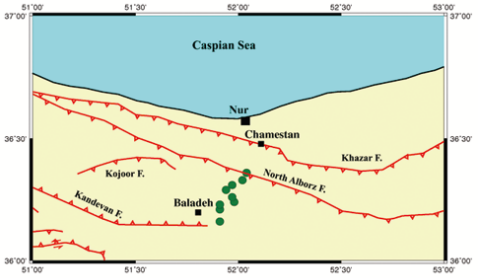

Fig. 3 Alborz and Khazar faults

Fig. 4 Surface section of Khazar fault

Fig. 5 Satelite map of North Alborz fault zone

Table 1 Active faults around the study area (Babol city)

Fault name	Type of fault	Distance from Babol city (km)	Fault length (km)
North Alborz	Thrust fault	44	300
Khazar	Thrust fault	16	550
Firouzabad	Thrust fault	85	112
Atari	Thrust fault	91	85
Astaneh	Thrust fault	93	75
Kandovan	Thrust fault	100	64
Mosha	Thrust fault	91	400
North of Tehran	Thrust fault	115	108
Firouzkooh	Thrust fault	84	40
Bayejan	Thrust fault	60	45
Damghan	Thrust fault	136	100
Orim	Thrust fault	72	44

Table 2 Recent major earthquakes around the study area (Babol city))

Earthquake	Magnitude	Depth (km)	Year
Chalus, Mazandaran	6.3	17	2004
Babol, Mazandaran	5.1	15	2012
Damghan, semnan	5.7	7	2010
Roudbar and Manjil	7.4	10	1990

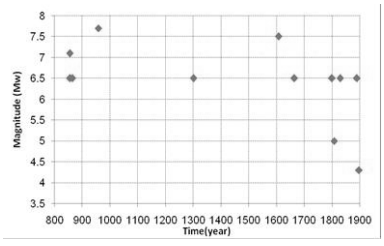

(a) Earthquakes of Babol from 800 to 1900

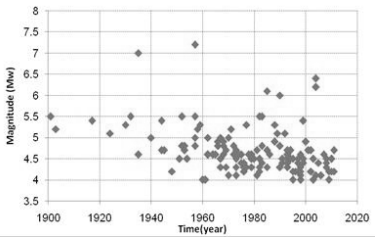

(b) Earthquakes of Babol from 1900 to 2014

Fig. 6 Magnitude distribution of earthquakes in the range of 200 km around the Babol city

Babolrud River originates in the Alborz mountains and is one of the major rivers in Iran. It is located on the left side of Babol city. The study area is con-

stantly filled with the new alluvial sediments of the Babolrud River. Following paragraphs provide an overview of the site investigation conducted at 35 km2 of Babol city and present the results of both geotechnical and geophysical investigations. Also, supplemental activities related to Babol seismic microzonation project are illustrated too.

Regarding to mentioned project, a total of 35 new boreholes have been drilled in study area. Also, the results of previous investigations (consist of 60 borholes) were collected too (Figure 7). The depth of boreholes ranged from 25 to 40 m. Downhole logging surveys and SPT tests carried out through new 35 boreholes, were performed at every 1.5 m and 2 m of depth. The location of drilled boreholes over Babol City, a sample of geotechnical test results and shear wave velocity profile obtained by downhole test are shown in Figure 8 and Figure 9.

The general topographic gradient in the study area is constant. During the investigation, the site soils were observed to consist of silty clay, silty sand and sandy clay. The depth of the water table as measured during drilling should be

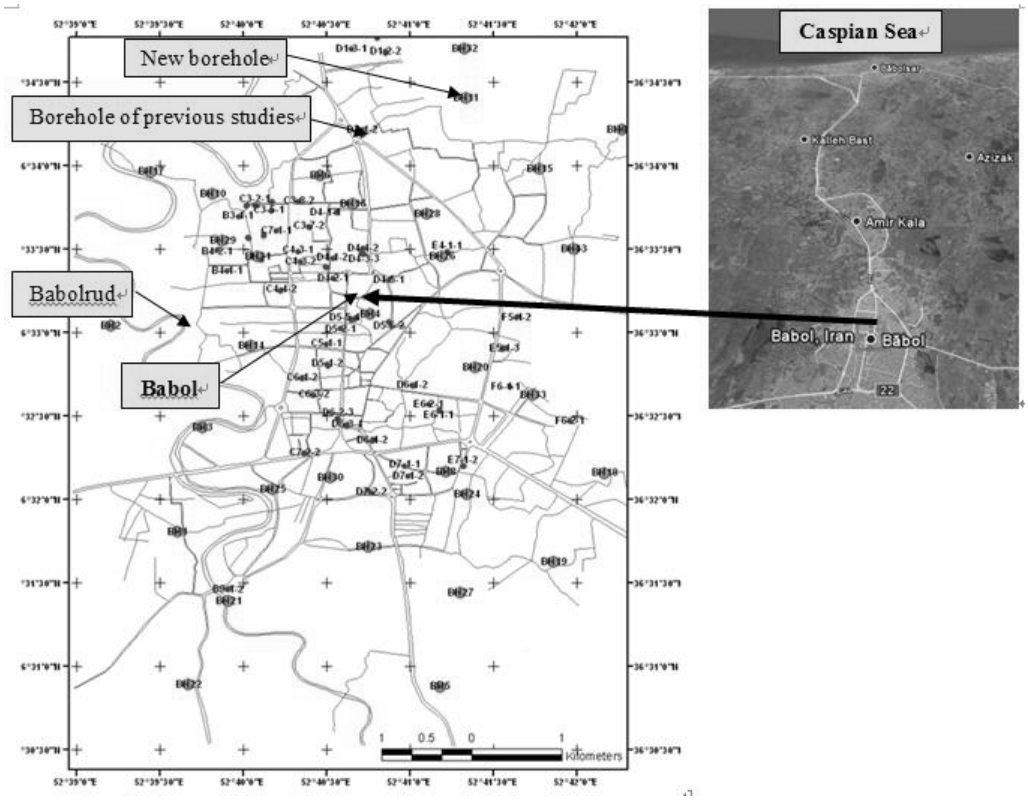

Fig. 7 Location of drilled boreholes over Babol city

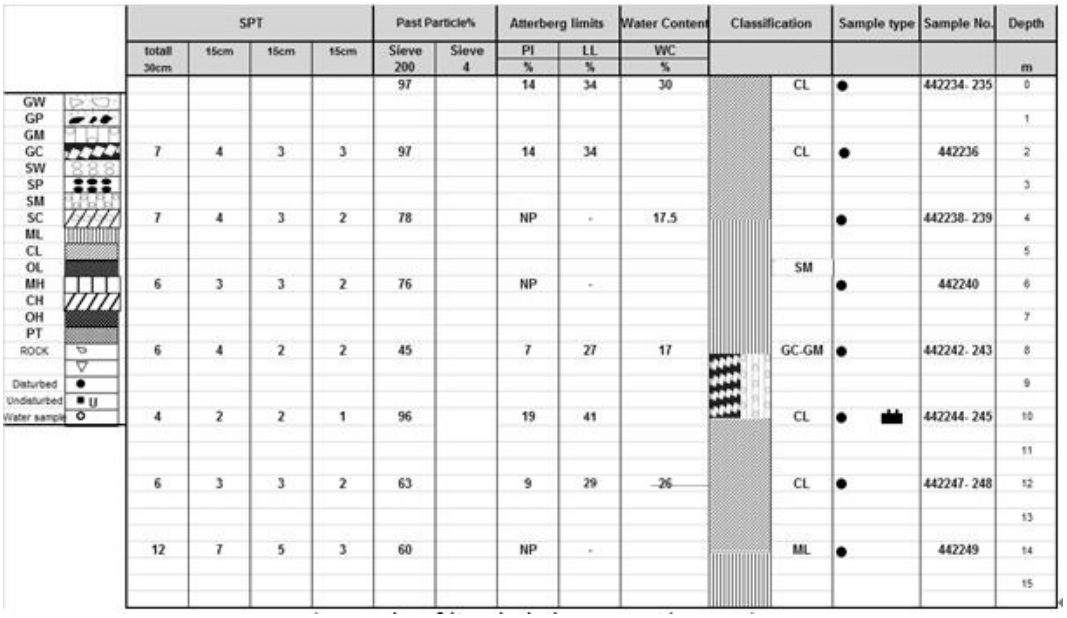

(a) Sample of borehole log report (0-15 m)

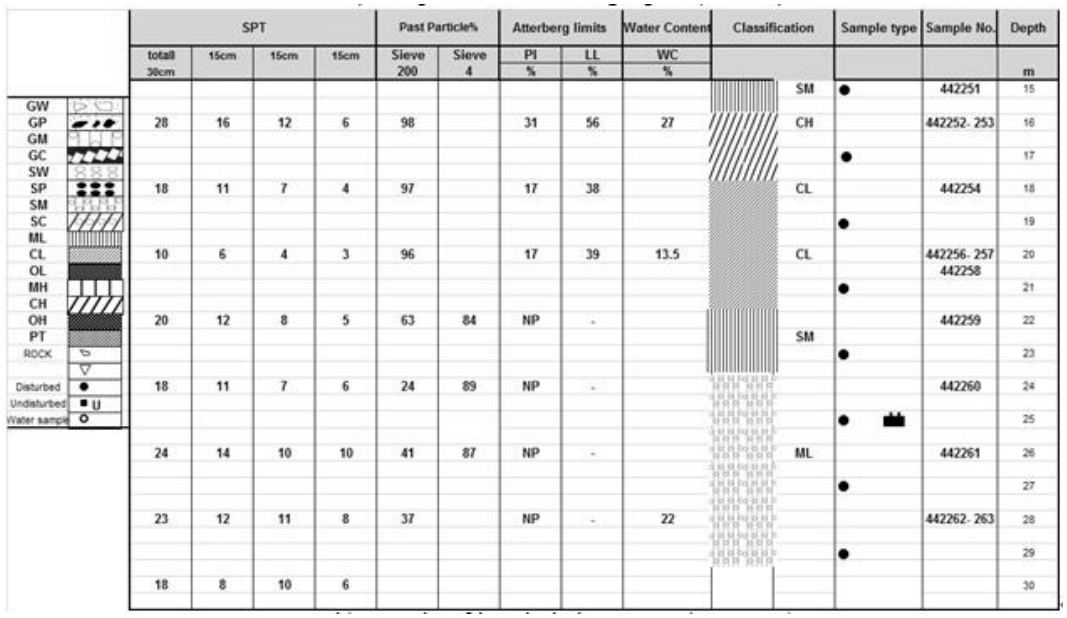

(b) Sample of borehole log report (15-30 m)

Fig. 8 results of laboratory and in-situ tests (geotechnical investigations)

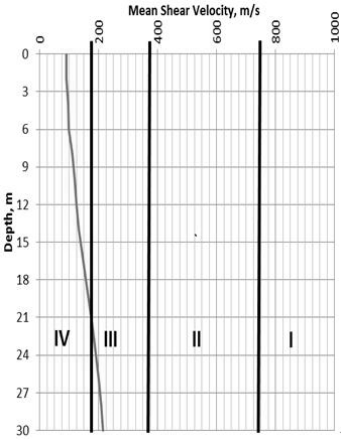

(a) Sample of shear wave velocity profile

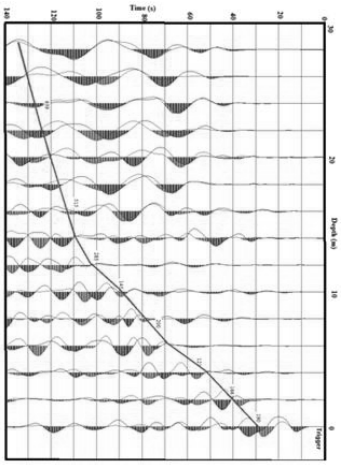

(b) Sample of S wave data obtained during downhole test

Fig. 9 Results of geophysical (downhole) surveys

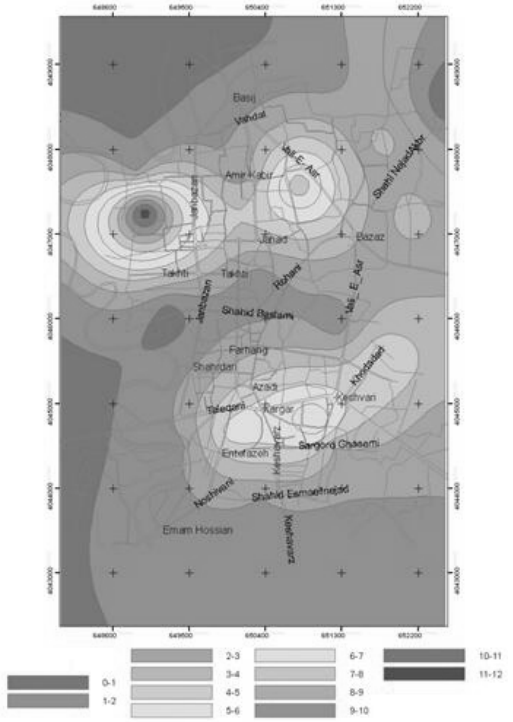

Fig. 10 Location of drilled boreholes over Babol city

carefully evaluated. It is always necessary to wait for at least 24 hours to check on the stabilized water table for the final measurement. Groundwater levels in areas of the Babol city is presented Figure 10 [36].

3 Results and Discussion

In reality, soil behaves as a deformable body instead of as a rigid body. As a result, the actual peak shear stress induced at each depth is less than that predicted in surface. Therefore, the rigid body shear stress should be reduced with depth reduction factor (r_d), to give the deformable body shear stress. The depth reduction factor (r_d) can be computed as follows (Equation 7) [37-38]:

$$r_d = \frac{(\tau_{max})_{depth}}{(\tau_{max})_{rigidboady}} = \frac{(a_{max})_{depth}}{(a_{max})_{surface}} \tag{7}$$

Amplification refers to the increase in the amplitudes of seismic waves as they propagate through the soil layers near the surface of the earth. This is because the ground under these districts is relatively soft. Soft soils usually, amplify ground shaking. Influence of the soil response on the seismic motion at the ground surface, is considered through the equivalent linear or nonlinear one-dimensional response of a soil column. These methods of analysis require selection and scaling of ground motions appropriate to design hazard levels. It is necessary to select empirical recordings of ground motion and scale these ground motions to the level of the design spectrum.

In order to develop the depth reduction factor (r_d), the max acceleration at surface and each depth should be calculated [39]. In this research, site response analyses, performed by the GeoStudio software, were carried out for 35 boreholes using 4 scaled earthquakes with 109, 475, 975 and 2500-year return period. The details of mentioned scaled accelerograms are presented in Table 3 and Figure 11. Finally the (r_d) diagrams for each zone of study area is drown and a new empirical correlation is proposed.

Table 3 Details of scaled earthquakes

Earthquake name	a max (g) - at bedrock	Return period (year)
Kareh-Bas	0.108	109
Bam	0.215	475
Northridge	0.302	950
San Fernando	0.364	2500

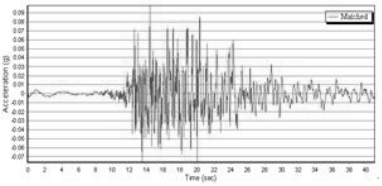

(a) Scaled time history records of the Kareh-Bas earthquake (109-year return period)

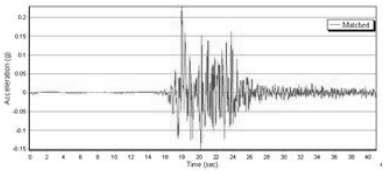

(b) Scaled time history records of the Bam earthquake (475-year return period)

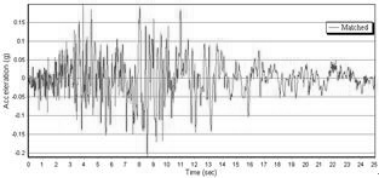

(c) Scaled time history records of the Northridge earthquake (950-year return period)

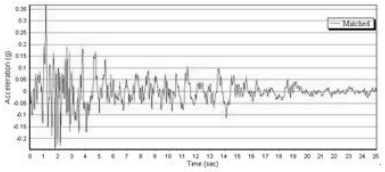

(d) Scaled time history records of the San Fernando earthquake (2500-year return period)

Fig. 11 Time history records of scaled earthquake for performing site response analyses

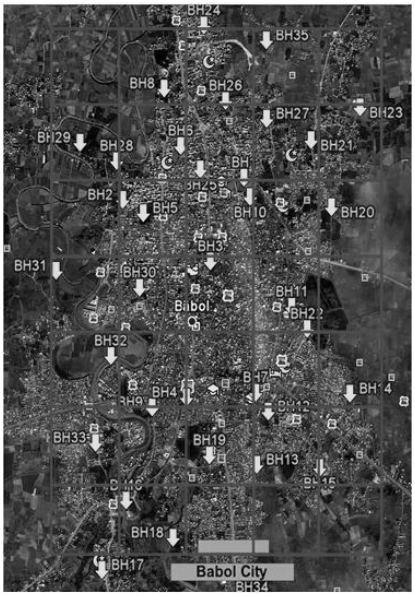

Fig. 12 35 zones of study area (site response analyses are performed for each zone)

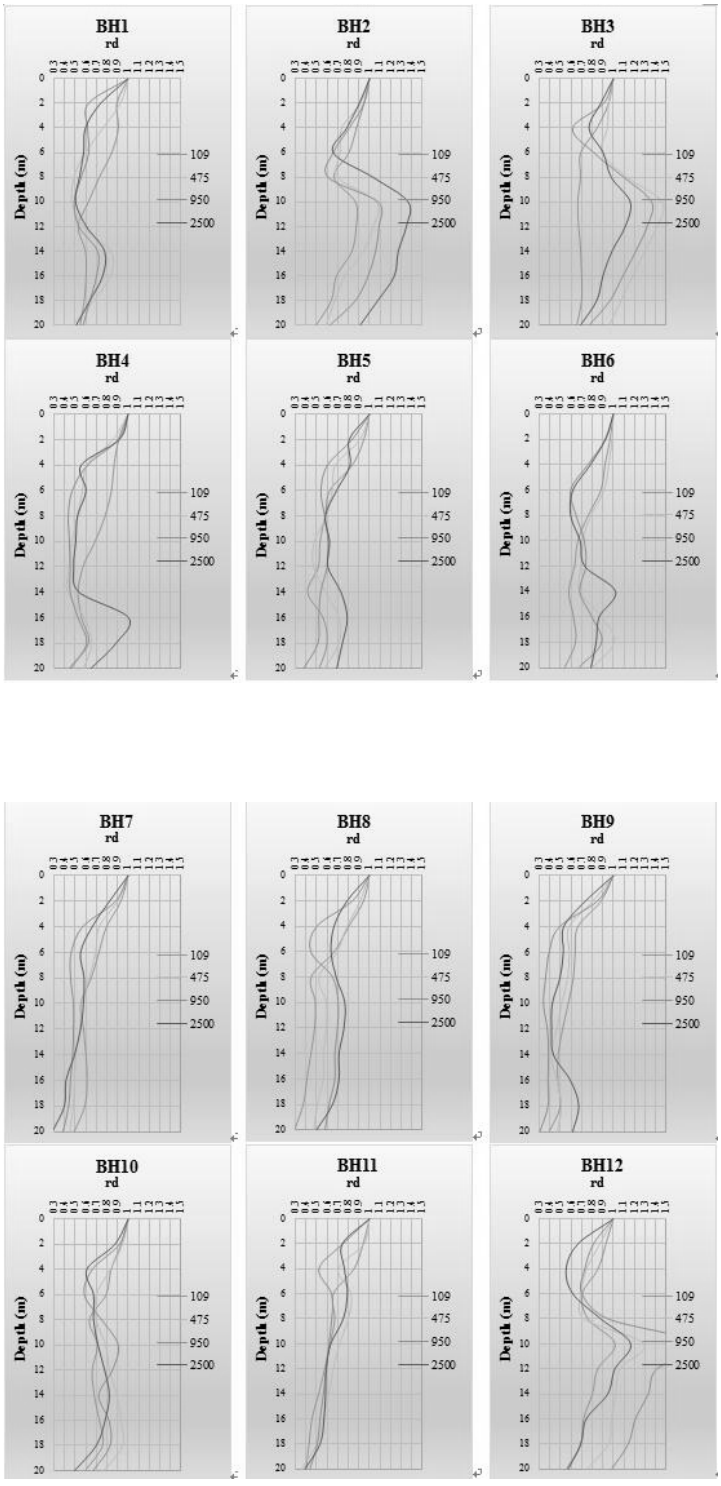
BH1
BH2
BH3
BH4
BH5
BH6
BH7
BH8
BH9
BH10
BH11
BH12
rd
Depth (m)
109
475
950
2500

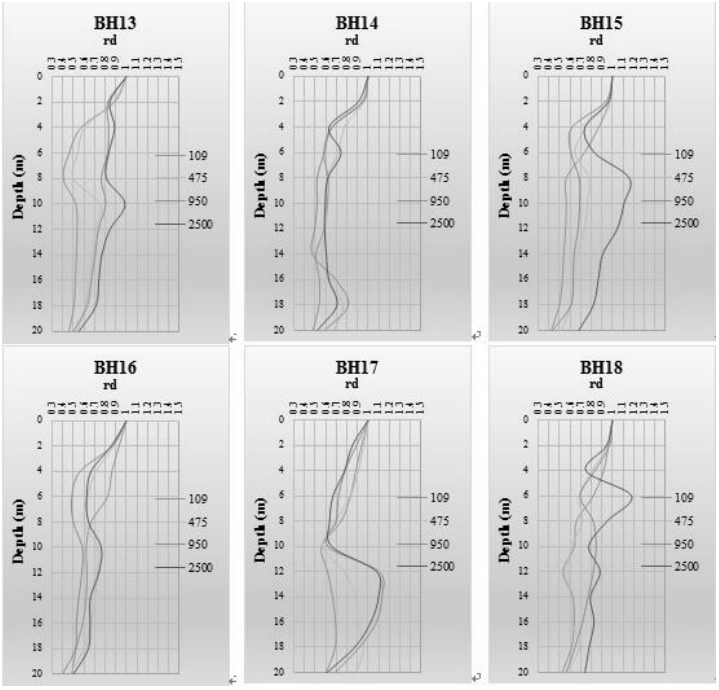
BH13
BH14
BH15
BH16
BH17
BH18
rd
Depth (m)
109
475
950
2500

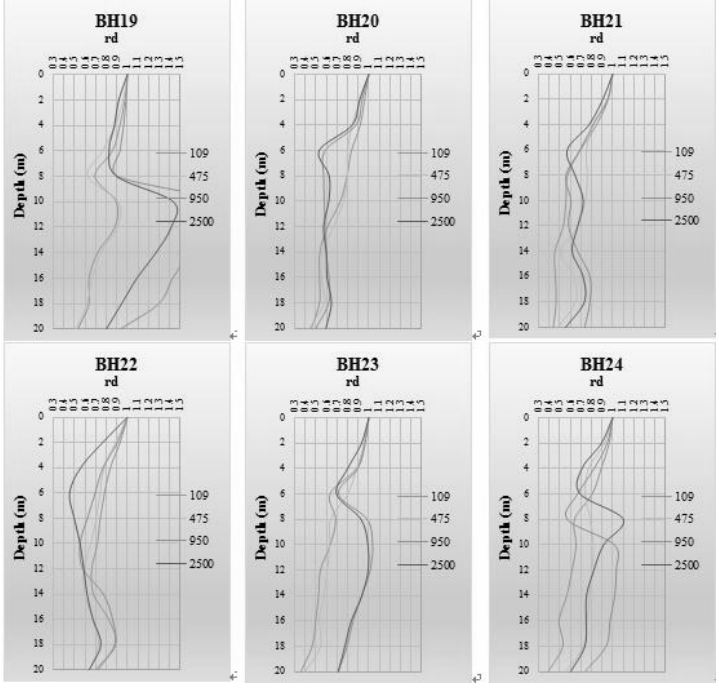
BH19
BH20
BH21
BH22
BH23
BH24
rd
Depth (m)
109
475
950
2500

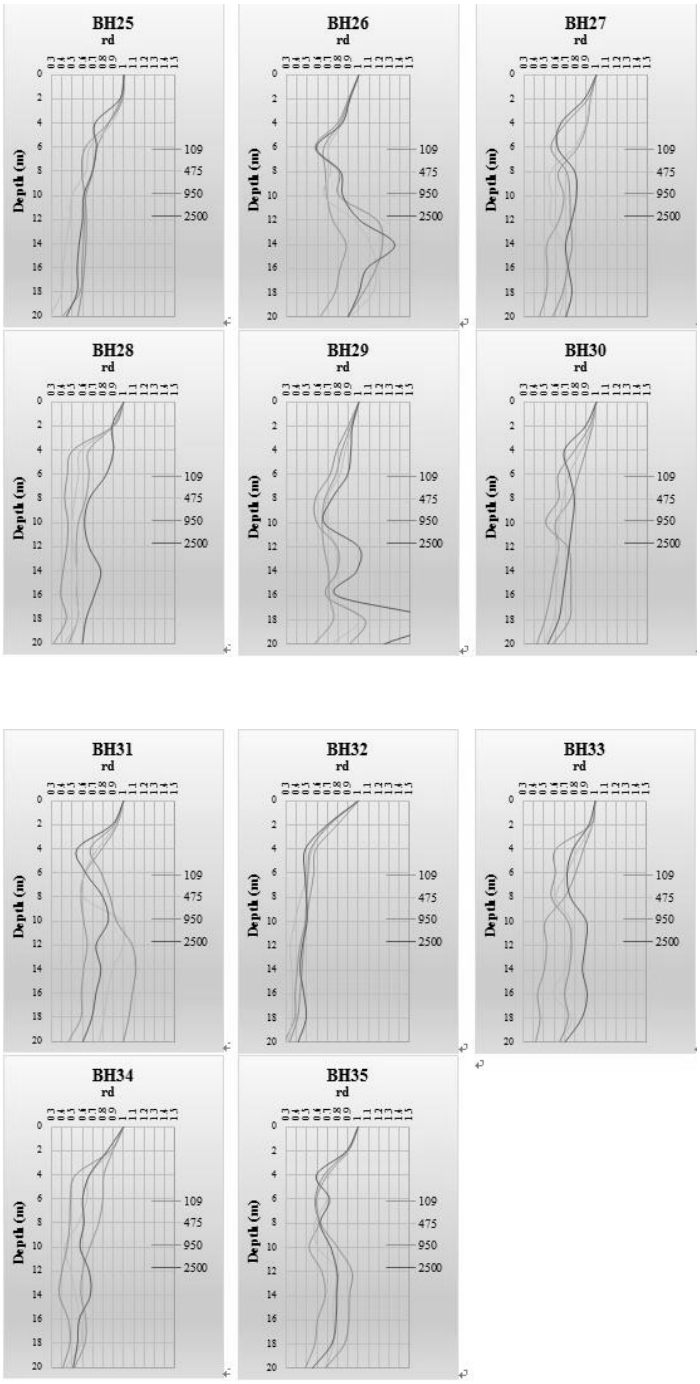

Fig. 13 Variations of the stress reduction coefficient (r_d) with depth for various zones of Babol city

In order to define the depth reduction factor for Babol city, 35 zones were each analyzed using scaled input motions (Figure 12). Then the rd diagrams were developed for each zone. Figure 13 shows the depth reduction factor for each zone based on different input motions.

Most researchers today agree that there is no correlation for assessment of depth reduction factor which can be applicable for different soil types and all regions. Different site conditions such as soil and sediment erosion, geological situation, soil structure and fabric, seismicity of area and ... are the main factors of mentioned uncertainty. So it can be said that the best empirical correlations for a specific region should be assessed regarding to in-situ tests and site response analyses which are performed in that region.

In this research, an empirical correlation is suggested based on more than 200 site response analyses for different zones of Babol city, using 4 scaled earthquake motions. The proposed new correlation for estimation of r_d as a function of depth is presented in Equation 8.

Table 4 Details of scaled earthquakes

$r_d = -0.0425z + 1.0333$	$0 \leq z \leq 6$	Equation 8
$r_d = 0.0006z^2 + 0.0048z + 0.7865$	$6 < z < 12$	
$r_d = -0.02z + 1.06$	$12 \leq z \leq 14$	
$r_d = 0.0025z^2 + 0.072z + 0.261$	$14 < z \leq 20$	

4 Conclusion

Liquefaction in soil is one of the major problems in geotechnical earthquake engineering. The simplified method of Seed and Idriss (1971) is the most common procedure used for evaluation of liquefaction potential. In mentioned simplified method, an empirical correlation was developed for estimation of r_d based on the 2153 site response analyses.

Previous developed r_d functions can be unconservative in comparison to actual case-specific seismic response analysis. Therefore, in places with high potential of liquefaction, the CSR is recommended to be calculated using a modified dynamic response analysis.

This research proposed the values of depth reduction factor (r_d) based on the results of several extensive site response analyses of Babol city at 35 zones. Firstly, 4 modified and scaled acceleration records (Kareh-Bas earthquake with 109-year return period, Bam earthquake with 475-year return period, Northridge earthquake with 975-year return period and San Fernando earthquake with 2500-year return period) were used as input motions at the bedrock of the 35 zones. Soil layers were idealized as horizontal layers. Engineering properties of each

layer, ground water level and other necessary data collected during geotechnical investigations and geophysical surveys were used to develop the soil column extending form the ground surface to bedrock. Then, local site effects of study area were evaluated numerically with equivalent linear method and finally the depth reduction factor (r_d) diagrams and correlation were prepared for study area.

In some cases, depending on geotechnical and geological situation of a site or seismicity of a study area, the CSR calculated by the simplified method could be incapable, overestimated or underestimated. To summarize it can be said that, the variation of CSR obtained by site response analysis could be considered more reliable. Also in complex and unusual sites or during strong shaking levels, it can be recommended that the more comprehensive alternative is to develop depth reduction factor based on site response analysis.

References

[1] Nguyen KH and Gatmiri B. (2007), "Evaluation of seismic ground motion induced by topographic irregularity", *Soil Dynamics and Earthquake Engineering*, Vol. 27, No. 2, pp. 183-188.

[2] Chavez-Garcia FJ, Raptakis D, Makra, K. and Pitilakis, K. (2000), "Site effects at euroseistest-II. Results from 2D numerical modeling and comparison with observations", *Soil Dynamics and Earthquake Engineering*, Vol. 19, No. 1, pp. 23-39.

[3] Chopra , A K (2001), *Dynamic of structures theory and application to earthquake engineering*, Prentice Hall.

[4] Frankel A. (1993), "Three-dimensional simulations of ground motions in the San Bernardino valley, California, for hypothetical earthquakes on the San Andreas fault", *Bulletin of the Seismological Society of America*, Vol.83, pp.1020-1041.

[5] Gueguen P, Chatelain JL, Guillier B et al. (1998), "Site effect and damage distribution in Pujili (Ecuador) after the 28 March 1996 earthquake", *Soil Dynamics and Earthquake Engineering*, Vol.15, No.5, pp.329-334.

[6] Youd TL, Idriss IM, Andrus RD et al. (2001), "Liquefaction resistance of soils. Summary report from the 1996 NCEER and 1998 NCEER/NSF workshops on evaluation of liquefaction Resistance of Soils.", *Journal of Geotechnical and Geoenvironmental Engineering* , Vol. 127, No. 10, pp. 817-833.

[7] Seed HB and Peacock WH (1971), "The procedure for measuring soil liquefaction characteristics", *Soil Mechanics and Foundation Division (ASCE)* , Vol. 97, pp. 1099-1119.

[8] Kramer SL (2008), *Evaluation of liquefaction hazards in washington state*, Ground Settlement.

[9] Zhou YG, Chen YM and Ke H (2005), "Correlation of liquefaction resistance with shear wave velocity based on laboratory study using bender element.", *Journal of Zhejiang University Science* , Vol. 6, No. 8, pp. 805-812.

[10] Youd TL and Perkins DM (1978) , "Mapping of liquefaction induced ground failure potential. ", *Geotechnical Engineering Division (ASCE)*, Vol.104, No. 4, pp. 433-446.

[11] Youd TL and Hoose SN (1977) , "Liquefaction susceptibility and geologic setting ", *Proceeding, 6th World Conference on Earthquake Engineering, Prentice-Hall, Englewood Cliffs*, Vol.3, No. 4, pp. 2189-2194.

[12] Wang W (1979), "Some findings in soil liquefaction", *Water Conservancy and Hydroelectric Power Scientific Research Institute*,Beijing.

[13] Robertson PK, Woeller DJ and Finn WD (1992), "Seismic cone penetration test for evaluating liquefaction potential under cyclic loading", *Canadian Geotechnical Journal*, Vol. 29, No. 3, pp. 686-695.

[14] Olsen RS, Youd TL and Idriss IM (1997), "Proceeding, NCEER Workshop on Evaluation of Liquefaction Resistance of Soils", *National Center for Earthquake Engineering Research*,State University of New York, Buffalo, pp. 225-276.

[15] Seed HB and Idriss IM (1971) , "Simplified procedure for evaluating soil liquefaction potential.", *Geotechnical Engineering Division (ASCE)* ,Vol. 97, No. 9, pp. 1249-1273.

[16] Seed RB, Cetin KO, Moss RE et al. (2003), *Recent advances in soil liquefaction engineering: a unified and consistent framework*, University of California, Berkeley.

[17] Seed HB (1979), "Soil liquefaction and cyclic mobility evaluation for level ground during earthquake", *Geotechnical Engineering Division (ASCE)*,Vol. 105, No. 2, pp. 201-255.

[18] Liao SS and Lum KY (1998), "Statistical analysis and application of the magnitude scaling factor in liquefaction analysis.", *Geotechnical Earthquake Engineering and Soil Dynamics*, Vol.1, pp. 410-421.

[19] Robertson PK and Wride CE (1998), "Evaluating cyclic liquefaction potential using the cone penetration test", *Canadian Geotechnical Journal*, Vol. 35, No. 3, pp. 442-459.

[20] Youd, T. L., Idriss, I. M. et al.(2001), "Liquefaction Resistance of Soils: Summary Report from the 1996 NCEER and 1998 NCEER/NSF Workshops on Evaluation of Liquefaction Resistance of Soils",*Journal of Geotechnical and Geoenvironmental Engineering*, Vol. 127, No. 10, pp. 817-833.

[21] Golesorkhi R (1989), *Factors influencing the computational determination of earthquake-induced shear stresses in sandy soils*, PhD dissertation, University of California at Berkeley.

[22] Cetin Ko, Seed RB, Kiureghian AD et al. (2004), "Standard penetration test-based probabilistic and deterministic assessment of seismic soil liquefaction potential.", *Journal of Geotechnical and Geoenvironmental Engineering*, Vol. 12, pp.1314-1340.

[23] Farrokhzad F, Choobbasti AJ, Barari A et al. (2011), "Assessing landslide hazard using artificial neural network: Case Study of Mazandaran, Iran.", *Carpathian Journal of Earth and Environmental Sciences*, Vol. 6, No. 1, pp. 251-261.

[24] Farrokhzad F, Choobbasti AJ and Barari A (2012), "Liquefaction micro-zonation of Babol city using artificial neural network.", *Journal of King Saud University (ELSEVIER)*, Vol. 24, No. 1, pp. 89-100.

[25] Farrokhzad F, Barari A, Ibsen LB et al. (2011), "Predicting subsurface soil layering and landslide risk with artificial neural networks: A Case Study from Iran", *Geologica Carpathica* , Vol. 62, No. 5, pp. 23-30.

[26] Kramer SL, Paulsen SB (2004), *Proceedings, International Workshop on Uncertainties in Nonlinear Soil Properties and their Impact on Modeling Dynamic Soil Response*, University of California, Berkeley.

[27] Kawano M, Asano K, Dohi H et al. (2010), "Verification of predicted non-linear site response during the 1995 Hyogo-Ken Nanbu earthquake.", *Soil Dynamics and Earthquake Engineering*, Vol. 20, No. 5, pp. 493-507.

[28] Godano C and Oliveri F (1998), "Nonlinear seismic waves: A model for site effects", *International Journal of Non-Linear Mechanics*,Vol. 34,pp. 457-468.

[29] Assimakia D and Kausel E (2002), "An equivalent linear algorithm with frequency- and pressure-dependent moduli and damping for the seismic analysis of deep sites", *Soil Dynamics and Earthquake Engineering*, Vol. 22, pp. 959-965.

[30] Choobbasti AJ, Rezaei S and Farrokhzad F (2013), "Evaluation of site response characteristic using microtremors", *Gradevinar*, Vol. 65, No. 8, pp. 731-741.

[31] Idriss IM and Seed HB (1968), "Seismic response of horizontal soil layers", *Journal of the Soil Mechanics and Foundations Division*, Vol. 94,pp. 1003-1031.

[32] Ishibashi I, Zhang X (1993), "Unified dynamic shear moduli and damping ratios of sand and clay", *Soils and Foundations*, Vol. 33, No. 1, pp182-191.

[33] Choobbasti AJ, Shooshpash E, Farrokhzad F (2012), "3-D Modeling of soils unsaturated depth using artificial neural network (Case Study of Babol)",*Unsaturated Soils: Research and Applications (SPERINGER)*, Vol. 2, pp. 317-324.

[34] Farrokhzad F, Barari A, Choobbasti AJ et al. (2011), "Neural network-based model for landslide susceptibility and soil longitudinal profile analyses: Two case studies",*Journal of African Earth Sciences (ELSEVIER)*, Vol. 61, pp. 349-357.

[35] Choobbasti AJ, Barari A, Safaie M et al. (2008), "Mitigation of Flourd (Pol e safid) landslide, northern Iran, using non-woven geotextiles", *Review of the Bulgarian Geological Society*, Vol. 69, No. 1, pp. 49-56.

[36] Choobbasti AJ, Shooshpasha E and Farrokhzad F (2013), "3-D Modeling of groundwater table using artificial neural network-case study of Babol", *Indian Journal of Geo-Marine Science*,Vol. 42, No. 7, pp. 903-906.

[37] Seed HB, Idriss IM and Arango I. (1983), "Evaluation of liquefaction potential using field performance data",*Journal of Geotechnical Engineering (ASCE)*, Vol. 109, No. 3, pp. 458-482.

[38] Seed HB and Lee KL (1966), "Liquefaction of saturated sands during cyclic loading", *Soil Mechanics and Foundations Division (ASCE)*, Vol. 92, pp. 105-134.

[39] Farrokhzad F, Choobbasti AJ and Barari A (2011), "Determination of liquefaction potential using artificial neural networks", *Gradevinar*,Vol. 63, pp. 837-845.

Corresponding author
Farzad Farokhzad can be contacted at: FarzadFarokhzad@mit.ac.ir